# ARF1 regulates the Rho/MLC pathway to control EGF-dependent breast cancer cell invasion

Sabrina Schlienger, Shirley Campbell, and Audrey Claing
Department of Pharmacology and Membrane Protein Research Group (GEPROM), Faculty of Medicine, Université de Montréal, Montréal, QC H3C 3J7, Canada

**ABSTRACT** **Invasion of tumor cells is a key step in metastasis that depends largely on the ability of these cells to degrade the extracellular matrix. Although we have showed that the GTPase ADP-ribosylation factor 1 (ARF1) is overexpressed in highly invasive breast cancer cell lines and that epidermal growth factor stimulation can activate this ARF isoform to regulate migration as well as proliferation, the role of this small GTP-binding protein has not been addressed in the context of invasiveness. Here we report that modulation of ARF1 expression and activity markedly impaired the ability of M.D. Anderson-metastatic breast-231 cells, a prototypical highly invasive breast cancer cell line, to degrade the extracellular matrix by controlling metalloproteinase-9 activity. In addition, we demonstrate that this occurs through inhibition of invadopodia maturation and shedding of membrane-derived microvesicles, the two key structures involved in invasion. To further define the molecular mechanisms by which ARF1 controls invasiveness, we show that ARF1 acts to modulate RhoA and RhoC activity, which in turn affects myosin light-chain (MLC) phosphorylation. Together our findings underscore for the first time a key role for ARF1 in invasion of breast cancer cells and suggest that targeting the ARF/Rho/MLC signaling axis might be a promising strategy to inhibit invasiveness and metastasis.**

**Monitoring Editor**
J. Silvio Gutkind
National Institutes of Health

Received: Jun 20, 2013
Revised: Oct 4, 2013
Accepted: Oct 30, 2013

## INTRODUCTION

Cell invasion is a process tightly regulated by multiple signaling proteins, such as plasma membrane receptors, adaptors, and small GTP-binding proteins. During cancer progression, transformed cells migrate and invade surrounding tissues to form metastasis. Expression of small GTPases and their regulatory factors is frequently modulated in human cancers (Karnoub and Weinberg, 2008; Vigil *et al.*, 2010; Mardilovich *et al.*, 2012). The ADP-ribosylation factor (ARF) family of proteins has been associated with cancer progression (Sabe *et al.*, 2009). We showed that the GTPase ARF1 is overexpressed in highly invasive cancer cells and that epidermal growth factor (EGF) stimulation can activate this ARF isoform to regulate migration (Boulay *et al.*, 2008; Lewis-Saravalli *et al.*, 2013).

Like all GTPases, ARFs cycle between their inactive (GDP bound) and active (GTP bound) form. This process is controlled by guanine nucleotide exchange factors (GEFs), which catalyze the exchange of GDP to GTP, and GTPase-activating proteins (GAPs), which accelerate the hydrolysis of bound GTP. Six ARF genes have been identified, and ARF1 and ARF6 are the best characterized. In invasive breast cancer cells, we reported that stimulation of the epidermal growth factor receptor (EGFR) activates ARF1 in order to regulate cell proliferation and migration by affecting the phosphoinositide 3-kinase (PI3K) pathway (Boulay *et al.*, 2008). In contrast, ARF6 regulates migration and invasion by activating the mitogen-activated protein kinase pathway (Hashimoto *et al.*, 2004; D'Souza-Schorey and Chavrier, 2006; Boulay *et al.*, 2008). GTPases of the Rho family, RhoA and RhoC, play a major role in several key steps of cancer progression, such as invasion (Simpson *et al.*, 2004). Depletion of RhoA or RhoC inhibits the invasiveness of M.D. Anderson-metastatic breast-231 (MDA-MB-231) cells (Pille *et al.*, 2005; Wu *et al.*, 2010). Positive correlation was reported between the expression level of RhoA and disease progression in breast cancer tumors (Fritz *et al.*, 2002). RhoC was also reported as a

This article was published online ahead of print in MBoC in Press (http://www.molbiolcell.org/cgi/doi/10.1091/mbc.E13-06-0335) on November 6, 2013.

Address correspondence to: Audrey Claing (audrey.claing@umontreal.ca).

Abbreviations used: ARF, ADP-ribosylation factor; EGF, epidermal growth factor; EGFR, epidermal growth factor receptor; MDA-MB-231, M.D. Anderson-metastatic breast-231; MLC, myosin light chain; MMP, metalloproteinase; PI3K, phosphoinositide 3-kinase; siRNA, small interfering RNA.

gene positively associated with metastasis (Suwa *et al.*, 1998; Clark *et al.*, 2000).

Breaching of the basement membrane is classically associated with invadopodia. These are actin- and cortactin-rich protrusions of the cell membrane that extend into the extracellular matrix (Weaver, 2006). Invadopodia contain metalloproteinases (MMPs) essential for proteolytic degradation of the matrix (Monsky *et al.*, 1994; Nakahara *et al.*, 1997). Cells can also invade their surrounding by releasing shedding microvesicles. These are now recognized as specific structures different from exosomes, as they bud directly from the plasma membrane into the extracellular space (Cocucci *et al.*, 2009; Muralidharan-Chari *et al.*, 2010). These plasma membrane–derived microvesicles are released from a large number of cell types, including fibroblasts, platelets, macrophages, and endothelial and tumor cells (Cocucci *et al.*, 2009). They display a variable spectrum of molecules specific to the parental cell that secretes them. They are believed to facilitate cell invasion by releasing proteases important for matrix degradation, such as MMPs (Dolo *et al.*, 1999; Taraboletti *et al.*, 2002). MDA-MB-231 cells express 26 MMP genes, and several of these are associated with increased invasiveness (Hegedus *et al.*, 2008).

Although we demonstrated that ARF1 is overexpressed in invasive breast cancer cells (Boulay *et al.*, 2008), the role of this ARF isoform in the invasion process remains unknown. Because ARF1 controls migration and proliferation (Boulay *et al.*, 2008, 2011), we reasoned that this ARF isoform is also a key signaling effector regulating invasion. Here we demonstrate that modulation of ARF1 expression levels and activity leads to impaired invasive capacities of MDA-MB-231 cells through invadopodia maturation and shedding of microvesicles. We define the molecular circuit that governs the invasion process by showing that ARF1 plays a critical role in modulating Rho-dependent signaling events leading to regulation of myosin light chain (MLC). Furthermore, we report that knockdown of ARF1 markedly inhibits maturation of invadopodia, release of shedding microvesicles, and MMP-9 activity. Our findings reveal, for the first time, the central role of ARF1 in breast cancer cell invasion and identify a putative new target for the development of anti–breast cancer therapies.

## RESULTS

### ARF1 controls invasion of MDA-MB-231 breast cancer cells

Using the prototypical highly invasive, triple-negative breast cell line MDA-MB-231, we first investigated the extent to which ARF1 controls invasiveness by examining gelatin degradation. Scrambled and ARF1-depleted cells were seeded onto fluorescently labeled, gelatin-coated coverslips. After 16 h, cells were fixed and actin stained using rhodamine–phalloidin. In control condition, gelatin degradation was observed by the decrease of green fluorescence under and around the cells. ARF1 knockdown by two different small interfering RNAs (siRNAs) reduced the ability of the cells to degrade the matrix by 56% (Figure 1A, Supplemental Figure S1A, and Supplemental Video S1). Gelatin degradation observed in ARF1 siRNA transfected cells was rescued by expression of the siRNA-resistant hemagglutinin (HA)-tagged ARF1 (Supplemental Figure S1A). Alternatively, increasing ARF1 levels did not significantly affect gelatin degradation. However, expression of a dominant-negative mutant, ARF1 $T^{31}N$, or a constitutively active mutant, ARF1 $Q^{71}L$, inhibited this response by 50%, suggesting that cycling of the small GTPase is important for downstream signaling leading to this response (Figure 1A and Supplemental Figure S1B). Cellular invasion is also classically assessed by Transwell migration through Matrigel. This laminin-, type IV collagen–, and growth factor–enriched matrix is widely used as a mimic of basement membrane. In such an assay, a 20-h EGF stimulation increased cell invasion by 2.1-fold. Depletion of ARF1 by RNA interference significantly reduced basal as well as EGF-stimulated invasion (Figure 1B). In this context, proliferation and migration were also inhibited by the depletion of ARF1, contributing to the overall effect observed (Supplemental Figure S1, C and D). Because malignant breast cells can be cultured within a three-dimensional matrix to mimic the in vivo microenvironment (Lee *et al.*, 2007), we also assessed the role of ARF1 on cellular phenotype in a more complex setting. Similar amounts of MDA-MB-231 cells transfected with scrambled or ARF1 siRNA were first suspended in Matrigel (Supplemental Figure S1E). After 5 d, control cells formed complex stellate structures that invaded into the extracellular matrix (Figure 1C, left). In contrast, cells depleted of ARF1 formed spheroid-shaped colonies similar to normal mammary epithelial cells (Figure 1C, right). Taken together, these data provide evidence that ARF1 may be a key factor regulating the invasive properties of breast cancer cells.

### Depletion of ARF1 inhibits MMP-9 activity

Because invasion is characterized by the proteolytic degradation of the extracellular matrix, we quantified the enzymatic activity released in the extracellular media since most MMPs are secreted and subsequently activated. Here we focused on MMP-9 and MMP-2, two gelatinases expressed in MDA-MB-231 cells. First, extracellular media from control (scrambled siRNA) and ARF1-depleted cells were collected, and MMP activity was assessed by zymography assay. In conditions in which MDA-MB-231 cells were transfected with a scrambled siRNA, EGF stimulation resulted in an increase of MMP-9 activity without affecting MMP-2 (Figure 2A). When ARF1 expression was knocked down, both basal and EGF-stimulated MMP-9 activities were markedly reduced. Furthermore, in these conditions, we observed the appearance of the pro-form of MMP-9 (here activated biochemically), suggesting that ARF1 can regulate MMP-9 cleavage (Figure 2A). To verify that the degradation observed is due specifically to MMPs, we used batimastat (BB-94), a broad-spectrum inhibitor known to reduce invasion of MDA-MB-231 cells (Brown, 1995; Kelly *et al.*, 1998). After treatment of the cells with this compound, all enzymatic activity was lost, confirming the specific effect of MMPs in this experiment (Figure 2A). In cell lysates, MMP-9 is found as the pro form, and depletion of ARF1 did not affect its expression as assessed by Western blot analysis (Figure 2B). However, we observed that pro-MMP-9 was strongly ubiquitinated in ARF1-depleted conditions compared with control (Figure 2B). In addition, mRNA levels were increased in cells transfected with the ARF1 siRNA (Figure 2C). These data suggest that in ARF1-depleted conditions, pro-MMP-9 expression levels remain the same because, although mRNA levels are increased, degradation of pro-MMP-9 through the ubiquitin-proteasomal pathway is also increased.

### ARF1 regulates invadopodia maturation and microvesicle shedding

To further understand how ARF1 controlled MMP-9 activity to mediate matrix proteolysis, we examined the two main structures associated with cellular invasion: invadopodia formation and release of microvesicles. First, ARF1 was not found to localize into invadopodia of MDA-MB-231 cells (unpublished data). This observation corroborates previous work (Hashimoto *et al.*, 2004). Furthermore, when plated onto gelatin, similar numbers of actin and cortactin-rich invadopodia were found in control and ARF1-depleted cells (Figure 3A), suggesting that ARF1 does not regulate the initial step of invadopodia formation. However, further analysis of the invadopodia, through *Z*-stack reconstructions, revealed that the structures present at the ventral surface of the cells transfected with the ARF1 siRNA

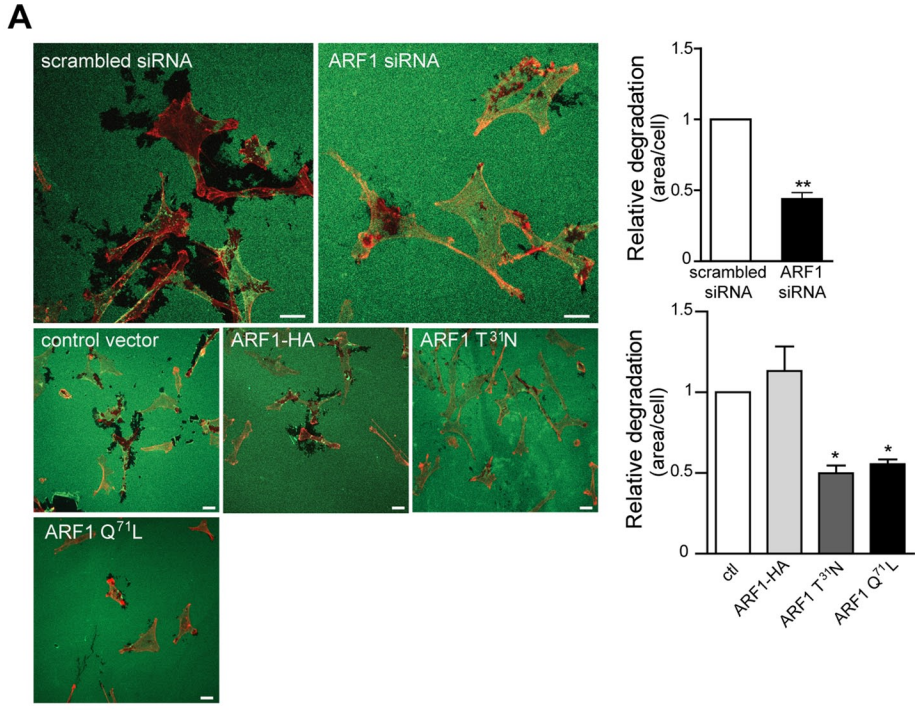


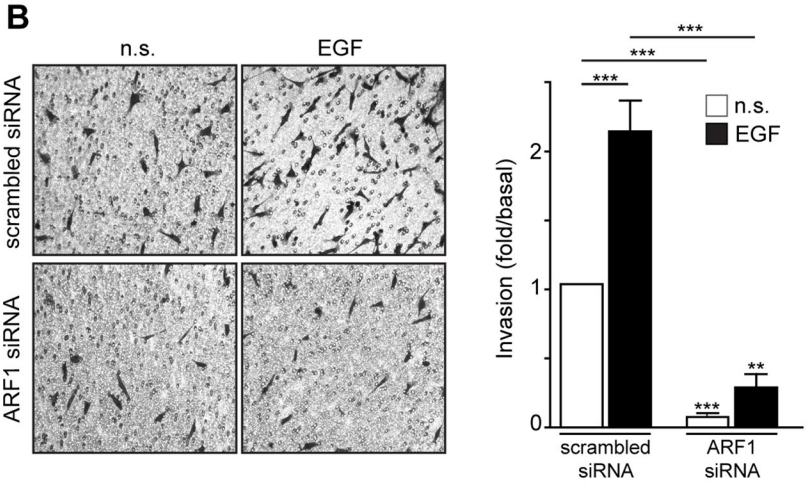


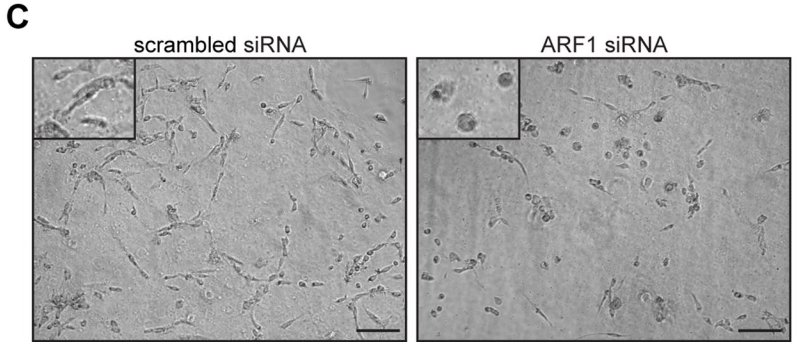


FIGURE 1: Modulation of ARF1 expression affects cell invasion. (A) Cells were transfected with a scrambled or ARF1 siRNA, empty vector (control), ARF1, ARF1 $T^{31}N$, or ARF1 $Q^{71}L$ and seeded onto Alexa Fluor 488–coupled gelatin. After 16 h, cells were fixed and actin stained using Alexa Fluor 568–phalloidin. Images are representative of three independent experiments with >100 cells examined per condition. Quantification of data are mean ± SEM of three experiments. *$p < 0.05$, ** $p < 0.01$; values are compared with control conditions. Scale bars, 20 μm. (B) MDA-MB-231 cells were transfected with a scrambled or ARF1 siRNA and seeded into Matrigel-coated Boyden chambers. Cells were left untreated (nonstimulated [n.s.]) or stimulated with EGF (30 ng/ml) for 20 h. Images are from the lower part of the Boyden chambers and are representative of three images taken per condition. Quantifications are mean ± SEM of five independent experiments. ***$p < 0.001$; values compared with the indicated condition. ARF1 level was assessed by Western blotting. (C) Cells were transfected as in A, and 48 h after transfection, they were seeded into Matrigel and allowed to proliferate for 5 d. Top left, magnifications showing four and three cells, respectively. Images are representative of three independent experiments with >100 cells examined per condition. Scale bars, 100 μm.

were smaller than the controls, suggesting that ARF1 may be essential for the final assembly and maturation steps of invadopodia (Figure 3A). To further address this issue, we examined the amount of Tks5 in invadopodia, since this adaptor protein is associated with the formation and maturation of these structures (Seals *et al.*, 2005; Stylli *et al.*, 2009; Murphy and Courtneidge, 2011). As illustrated in Figure 3B, Tks5 was enriched in control cells colocalizing with actin at invadopodia. However, in ARF1-depleted cells, the presence of Tks5 was reduced by 36%. These findings suggest an important role for ARF1 in the maturation of these structures (Figure 3B).

Shedding microvesicles released by MDA-MB-231 cells can be isolated by differential centrifugations of the culture media. It was reported that these vesicles, ranging from 300 to 900 nm, are present in the 10,000 × *g* fraction (Muralidharan-Chari *et al.*, 2009). As illustrated in Figure 4, Western blot analysis revealed that ARF1 was present in that 10,000 × *g* fraction of MDA-MB-231 culture media. Ultrastructural analysis by electron microscopy confirmed the previously reported heterogeneity of these microvesicles (Supplemental Figure S2). Furthermore, immunolabeling of the whole-mount preparations confirmed that ARF1 was present within these structures and mainly associated with the membranes (Figure 4A and Supplemental Figure S2). Depletion of ARF1 inhibited the release of plasma-derived microvesicles by 32% as assessed by total amount of proteins present in the 10,000 × *g* fraction (Figure 4B). Treatment with inhibitors of MLC pathway, such as ML-7, a myosin light-chain kinase inhibitor, or (–)-blebbistatin, a myosin II inhibitor, also inhibited the release of plasma-derived microvesicles (Figure 4B). We next examined the proteolytic activity associated with these microvesicles. We observed that MMP-9 activity was diminished in ARF1-depleted conditions (Figure 4C, left). However, we found no significant effect of ARF1 depletion on the amount of MMP-9 or MMP-2 in vesicle lysates (Figure 4C, right).

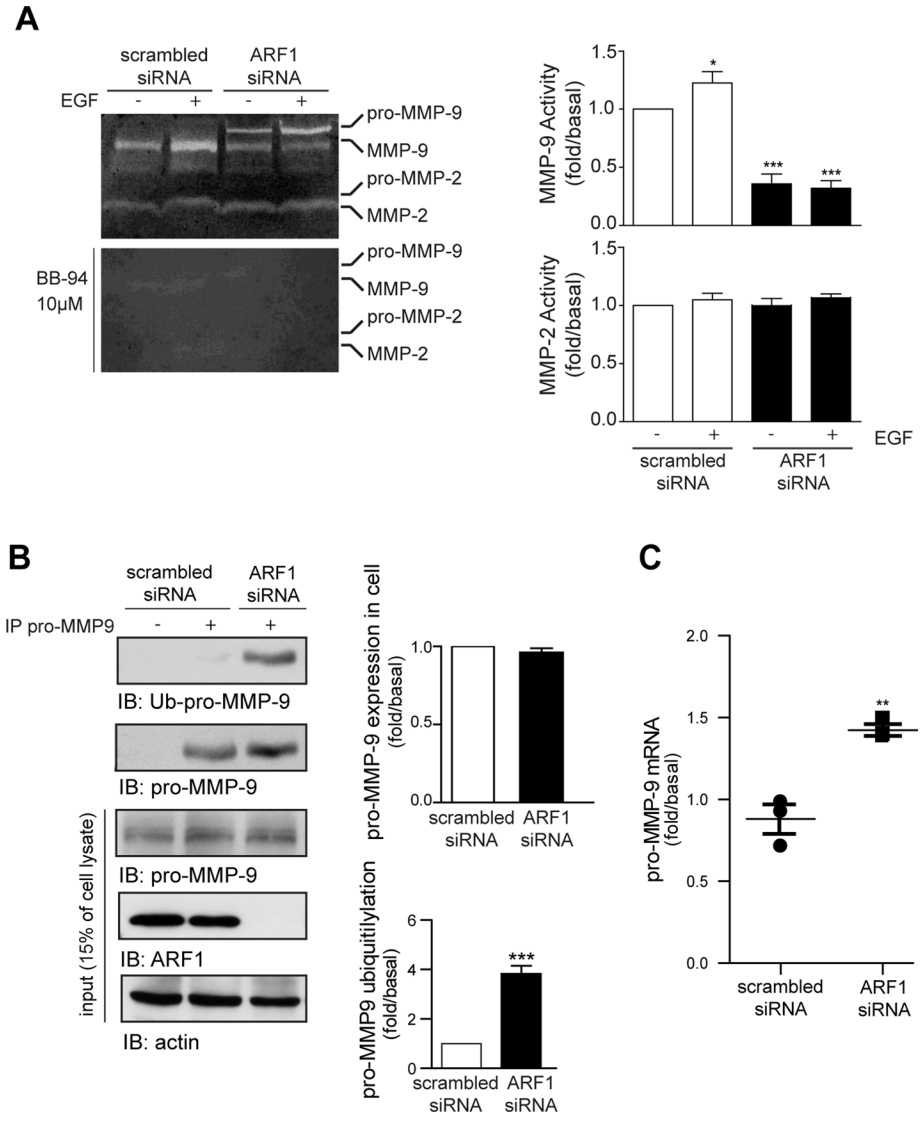


FIGURE 2: Modulation of ARF1 expression and MMP-9 activity. (A) MDA-MB-231 cells seeded in six-well plates were transfected with either scrambled or ARF1 siRNA. At 72 h later, cells were deprived of serum. Cells were stimulated or not for 12 h with EGF (100 ng/ml). Supernatants were collected and analyzed by zymography. A broad-spectrum inhibitor, batimastat (BB-94; 10 μM), was use to confirm the specific effect of MMPs. This experiment is representative of four others. Quantification is mean ± SEM of five independent experiments. *$p < 0.05$, ***$p < 0.001$. (B) Cells were transfected with control siRNA or siRNA against ARF1, and pro-MMP-9 was immunoprecipitated using a specific antibody. Levels of pro-MMP-9, ARF1, actin, and ubiquitinylation was detected using specific antibodies. Middle, quantification of the levels of pro-MMP-9 and pro-MMP-9 ubiquitination as determined by Western blot analysis of whole-cell extracts. Quantifications are mean ± SEM of five experiments. ***$p < 0.001$. (C) Cells were transfected as in A, and total RNA was extracted from MDA-MB-231 with TRIzol reagent. Right, pro-MMP-9 mRNA, is representative of three experiments performed in triplicate. **$p < 0.01$.

Together these data suggest that ARF1 may regulate matrix degradation by directly acting on the structures associated with invasiveness—invadopodia maturation and the shedding of membrane-derived microvesicles.

### ARF1 is necessary for the activation of MLC, which depends on the activation of RhoA and RhoC

Invadopodia activity, as well as microvesicle shedding, requires the phosphorylation of MLC (Alexander *et al.*, 2008; Muralidharan-Chari *et al.*, 2009). Inhibition of MLCK or myosin II by ML-7 and (–)-blebbistatin, respectively, has been shown to eliminate invadopodia-associated degradation (Alexander *et al.*, 2008). Furthermore, phosphorylation of MLC on Thr-18/Ser-19 residues is a step known to promote contraction of the actin-based cytoskeleton and generate the force required for microvesicle fission (Muralidharan-Chari *et al.*, 2009). We therefore next sought to investigate whether ARF1 could regulate MLC phosphorylation. As illustrated in Figure 5A, EGF stimulation of MDA-MD-231 cells transfected with a scrambled siRNA led to sustained phosphorylation of MLC on Thr-18/Ser-19 residues. After 60 min of stimulation, phosphorylation of MLC was 2.5-fold greater than baseline, reflecting potent activity of the protein. ARF1 knockdown completely abolished EGF-induced activation of MLC to the baseline level (Figure 5A). Of interest, ARF1 was not found in complex with MLC (unpublished data). Given that MLC phosphorylation is regulated by the Rho and Rho-associated kinase signaling axis (Amano *et al.*, 1996; Kimura *et al.*, 1996), we examined whether, in invasive breast cancer cells, RhoA and RhoC controlled the activation of MLC. As illustrated in Figure 5, B and C, depletion of either RhoA or RhoC completely abrogated phosphorylation of MLC. Of interest, knockdown of RhoC, but not of RhoA, inhibited MLC expression, suggesting that this isoform may regulate the function of MLC at the transcriptional level.

Because we previously reported that ARF proteins can directly interact and modulate the activity of the small GTP-binding protein Rac1 (Cotton *et al.*, 2007; Lewis-Saravalli *et al.*, 2013), we hypothesized that ARF1 might act to control the activation of other GTPases such as RhoA and RhoC, thereby modulating MLC phosphorylation. First, RhoA and RhoC activation was assessed upon EGF treatment of MDA-MB-231 cells. Rapid activation of both Rho isoforms was observed after 1 min of stimulation (Figure 6A and Supplemental Figure S3), followed by a sustained second phase of activation at 15 min (Figure 6B). This second peak remained elevated after 1 h of stimulation, as previously reported by other groups (Molli *et al.*, 2008; Gilcrease *et al.*, 2009). Depletion of ARF1 markedly reduced the activation of both small G proteins at the early and sustained time points (Figure 6, A and B, and Supplemental Figure S3). To exclude the possibility of off-target effects of the ARF1 siRNA, we undertook rescue experiments. As shown in Supplemental Figure S3, when expressed in ARF1-depleted cells, siRNA-resistant, HA-tagged ARF1 construct was able to rescue RhoA and RhoC activity. Of importance, the effect of ARF1 depletion on RhoA/C activity was also observed in two other invasive breast cancer cell lines, SKBR3 and HCC70 (Supplemental Figure S4). Rho activation is also characterized by

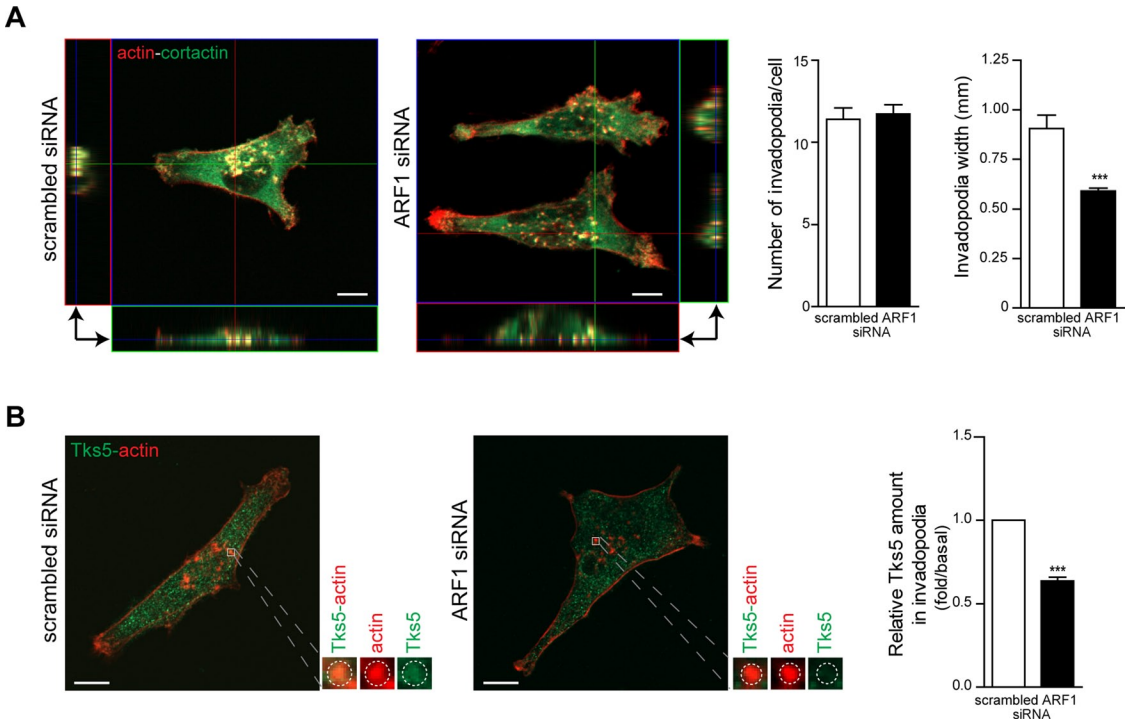


FIGURE 3: ARF1 depletion blocks invadopodia maturation. (A) Cells were transfected with scrambled or ARF1 siRNA and seeded onto nonfluorescent gelatin. After 16 h, cells were fixed and stained for actin and cortactin to visualize invadopodia. Cross sections were further analyzed through *Z*-stack. Images are representative of three independent experiments, with >50 cells examined per condition. Scale bars, 10 μm. Quantification of invadopodia number is representative of 30 cells from three independent experiments. Quantification of invadopodia width is representative of eight invadopodia in five cells per condition from three independent experiments. ***$p < 0.001$. (B) Cells were prepared as in A and stained for actin and Tks5 to assess invadopodia maturation. Scale bars, 10 μm. Quantification of Tks5 amount in invadopodia is representative of five invadopodia in five cells per condition from three independent experiments. ***$p < 0.001$.

the translocation of these GTPases to the plasma membrane (Yonemura *et al.*, 2004; Huveneers and Danen, 2009). In EGF-stimulated conditions, both RhoA and RhoC were enriched in membrane fractions at the corresponding maximal time points of their activation. In cells transfected with ARF1 siRNA, this biological response was dampened (Figure 6C and Supplemental Figure S5).

Alternatively, we assessed whether Rho GTPases could regulate the activation of ARF1. Our data show that depletion of neither RhoA nor RhoC significantly affected the early activation phase of ARF1 (Figure 7A). Longer exposure to the growth factor promoted a second phase of GTP loading on ARF1, which appeared at 5 min and was sustained for >30 min (Figure 7B). Depletion of RhoA or RhoC, however, markedly reduced this second burst of ARF1 activation, suggesting that Rho GTPases have the potential to regulate ARF1 activation. To further determine whether EGF stimulation is required for Rho to modulate ARF1 activity, we overexpressed Rho mutants mimicking the active form of the GTPases and examined ARF1-GTP levels. As depicted in Supplemental Figure S6A, overexpression of RhoA $Q^{63}L$ or RhoC $G^{14}V$ did not enhance levels of active ARF1, demonstrating that EGF-dependent signaling events are necessary for activation of this small G protein. We also found that overexpression of constitutively active ARF1 $Q^{71}L$ decreases RhoA and RhoC activation (Supplemental Figure S6B), further supporting the role of ARF1 $Q^{71}L$ in gelatin degradation. The exact role of both phases of ARF1 and RhoA/C activation remains to be elucidated. In sum, our data support a role for ARF1 as an upstream regulator of RhoA and RhoC.

To further investigate how ARF1 controlled Rho proteins, we sought to define whether these two classes of GTPases could be found in complex. Using coimmunoprecipitation assays, ARF1 was found associated with both RhoA and RhoC after EGF stimulation of MDA-MB-231 cells. The interaction was rapid and transient, with an early peak (1 min) and a later, more sustained phase (Figure 8A), similar to what we observed for their maximal activation times. Furthermore, we assessed whether RhoA and RhoC could also be present in shedding microvesicles. Western blot analysis showed that both GTPases were enriched in the 10,000 × g fraction (Figure 8B). Of interest, when RhoA and RhoC were immunoprecipitated from microvesicle lysates, they were found to interact with ARF1 (Figure 8C). Because ARF1 is not present in invadopodia, we did not investigate the ability of ARF1 and Rho GTPases to interact in these structures.

To demonstrate that the effects observed in ARF1 depleted cells depended on Rho GTPases, we attempted to rescue the phenotypes with the active Rho mutants. It was previously reported that RhoA activation was important for microvesicle formation in human cancer cells stimulated by EGF (Li *et al.*, 2012). As illustrated in Figure 9A, the expression of either RhoA $Q^{63}L$ or RhoC $G^{14}V$ alone or in combination was able to rescue the effect of ARF1 depletion on microvesicles shedding. Furthermore, expression of dominant-negative Rho mutants reduced microvesicle shedding (Figure 9B). Similar conditions were used to examine invasion. Overexpression of dominant-negative RhoA and RhoC mutants, independently or together, significantly inhibited invasion in the Matrigel-coated

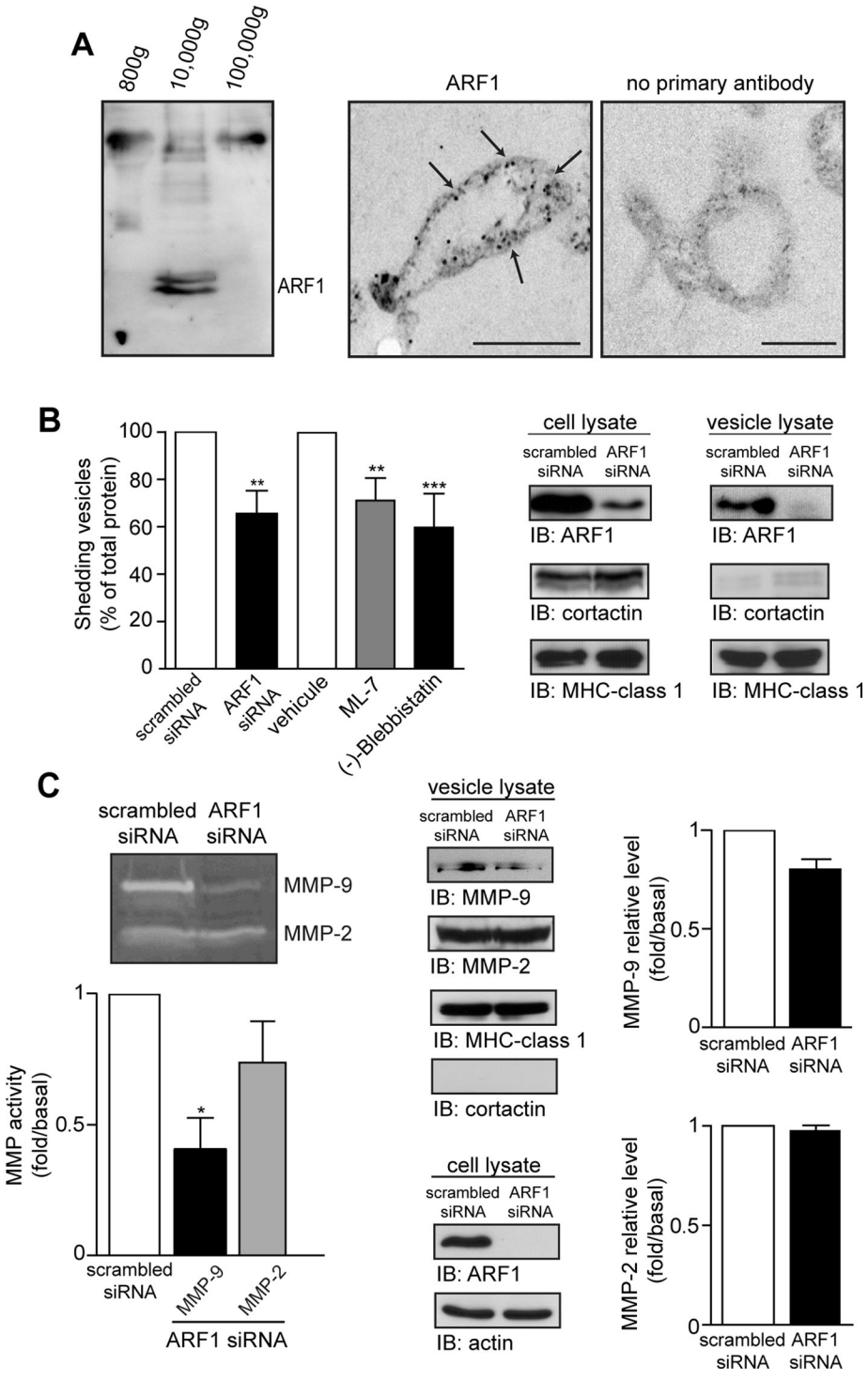


FIGURE 4: ARF1 is found in shedding microvesicles and controls their release. (A) Cell culture medium was collected and centrifuged to isolate shedding vesicles. Samples of each fraction were analyzed by Western blot, and the presence of endogenous ARF1 protein was observed in the 10,000 × *g* fraction. This experiment is representative of three others (left). Shedding microvesicles isolated by differential centrifugations were embedded in Epon and examined by electron microscopy (right). The electron microscopy image on the left shows vesicles positive for ARF1, and the image on the right is the negative control (no ARF1 antibody). Scale bars, 250 nm. These images are representative of 30 others taken from three independent experiments (10 images per experiment). (B) Cells were transfected with a scrambled or ARF1 siRNA or treated with a vehicle, ML-7 (10 μM), or (–)-blebbistatin (100 μM) overnight and shedding microvesicles isolated as in A. Quantification of shedding microvesicles was performed by measuring protein content in both conditions (left). Depletion of ARF1 and level of endogenous cortactin and MHC class I was confirmed by Western blot. Results are the mean ± SEM of five independent experiments. $^{**}p < 0.01$ and $^{***}p < 0.001$; values compared with the control or vehicle condition. (C) Microvesicle lysates were prepared from cells transfected with a scrambled or ARF1 siRNA and subjected to zymography (left) or Western blot (right). The levels of MMP-9, MMP-2, cortactin, and MHC-class I were determined by Western blot using specific antibodies. Bottom, levels of ARF1 and actin in the whole-cell extracts detected by Western blot. Results are mean ± SEM of five experiments. $^{*}p < 0.05$; values compared with the control condition.

Boyden chamber assay. In contrast, expression of the constitutively active mutants had the opposite effect. In conditions in which ARF1 expression was knocked down, overexpression of RhoA and RhoC active mutants rescued invasion (Figure 9C and Supplemental Figure S7).

Taken together, our findings suggest that ARF1 is the first upstream GTPase activated by EGFR and that this event is necessary for RhoA/RhoC activation and subsequent phosphorylation of MLC.

## DISCUSSION

In recent years, the role of ARF proteins in controlling key physiological responses of breast cancer cells has come to light. We showed that ARF1 and ARF6 are overexpressed in highly invasive tumor cell lines (Boulay *et al.*, 2008). Although much focus has been put on ARF6, the importance of the role of ARF1 in tumorigenesis is beginning to be recognized. The findings presented here demonstrate that ARF1 is a key player in breast cancer cell invasiveness and provide a mechanism by which this small GTPase controls this process.

ARF1 is mostly known for its role in the regulation of the secretory pathway. However, the demonstration that this ARF isoform is present at the plasma membrane and activated after receptor stimulation provides a new rationale for its role in different receptor-mediated biological functions (Cohen *et al.*, 2007; Boulay *et al.*, 2008). We showed that ARF1 controls breast cancer cell migration through regulation of the PI3K pathway and proliferation by regulating the function of pRB (Boulay *et al.*, 2008, 2011). Here we further provide evidences that these two key physiological responses are inhibited by ARF1 knockdown. Most important, we provide new evidence that ARF1 also controls invasiveness. A role for ARF proteins in regulating MMP activity has been suggested. Increasing concentrations of brefeldin A (BFA)

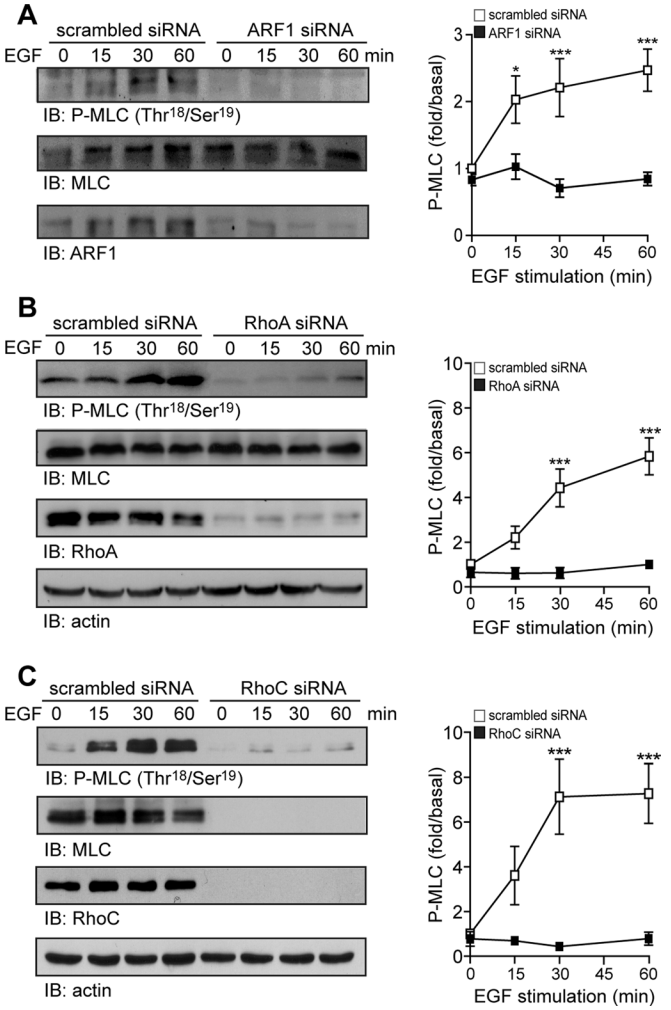


FIGURE 5: ARF1, RhoA, and RhoC control the phosphorylation of MLC upon EGF treatment. (A) MDA-MB-231 cells transfected with a scrambled or ARF1 siRNA were stimulated with EGF (100 ng/ml) for the indicated times. Endogenously expressed MLC (phosphorylated and total) and ARF1 were detected by Western immunoblotting using specific antibodies. Quantifications are mean ± SEM of four independent experiments. (B, C) Cells were transfected with a scrambled, RhoA, or RhoC siRNA. As in A, P-MLC, MLC, and ARF1 were detected by Western blotting. Data are mean ± SEM of three experiments. *$p < 0.05$, **$p < 0.01$, ***$p < 0.001$; values compared with control siRNA condition.

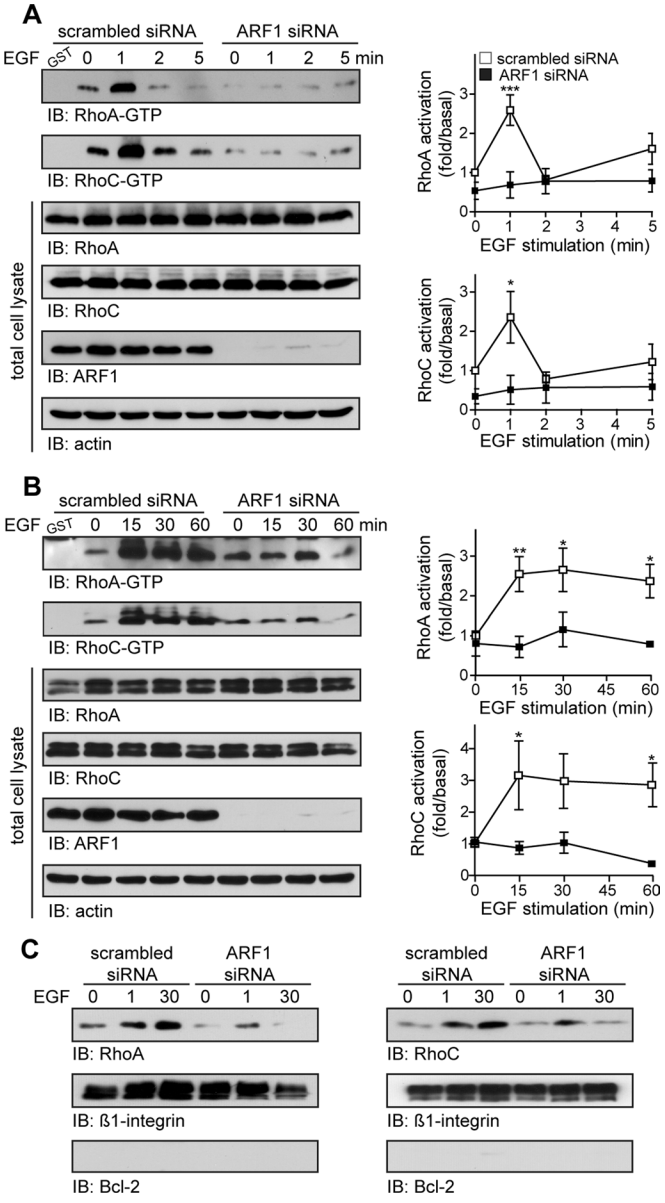


FIGURE 6: ARF1 controls Rho GTPases activation and localization. (A, B) Cells transfected with scrambled or ARF1 siRNA were stimulated with EGF (100 ng/ml) for the indicated times. Rho-GTP levels were assessed by Western blot analysis. Levels of ARF1, RhoA, RhoC, and actin protein were also determined by Western blot. (A) Early time points of EGF stimulation. Data are mean ± SEM of three experiments. (B) Longer time points of EGF stimulation. Data are mean ± SEM of three to five experiments. *$p < 0.05$, **$p < 0.01$, ***$p < 0.001$; values compared with nonstimulated control siRNA conditions. (C) Control (scrambled siRNA) and ARF1-depleted cells were stimulated with EGF (100 ng/ml) for the indicated times. Membrane fractions were prepared as described in *Materials and Methods*, and associated RhoA and RhoC were assessed by Western blotting. These experiments are representative of three and five others. β1-Integrin was used as a marker of plasma membrane and Bcl-2 as a marker of cytosol.

were reported to inhibit phorbol 12-myristate 13-acetate (PMA)-induced secretion of MMP-9 from HT 1080 fibrosarcoma cells (Ho *et al.*, 2003). Further analysis revealed that expression of a dominant-negative mutant form of ARF1 inhibited MMP-9 secretion by 22%. Our findings demonstrate that another BFA-sensitive ARF isoform, ARF1, also regulates MMP-9 activity in tumor cells. Analysis showed that pro-MMP-9 expression was similar in control and ARF1-depleted conditions. However, the level of active MMP-9 in both the basal and EGF-stimulated conditions was markedly reduced in ARF1-knockdown cells, suggesting a key role of this ARF in the activation process. In contrast to approaches that resulted in both MMP-9 and MMP-2 inhibition (Li *et al.*, 2011), ARF1 depletion selectively blocked MMP-9, demonstrating specificity of this GTPase toward a particular MMP. Whether ARF1 regulates the activity of other proteases remains to be examined.

Proteolytic degradation of the basement membrane by MMP is dependent on the formation of membrane protrusions and/or release of membrane-derived microvesicles, the two key structures associated with proteolytic degradation of the extracellular matrix. In this study, we demonstrate that depletion of ARF1 markedly

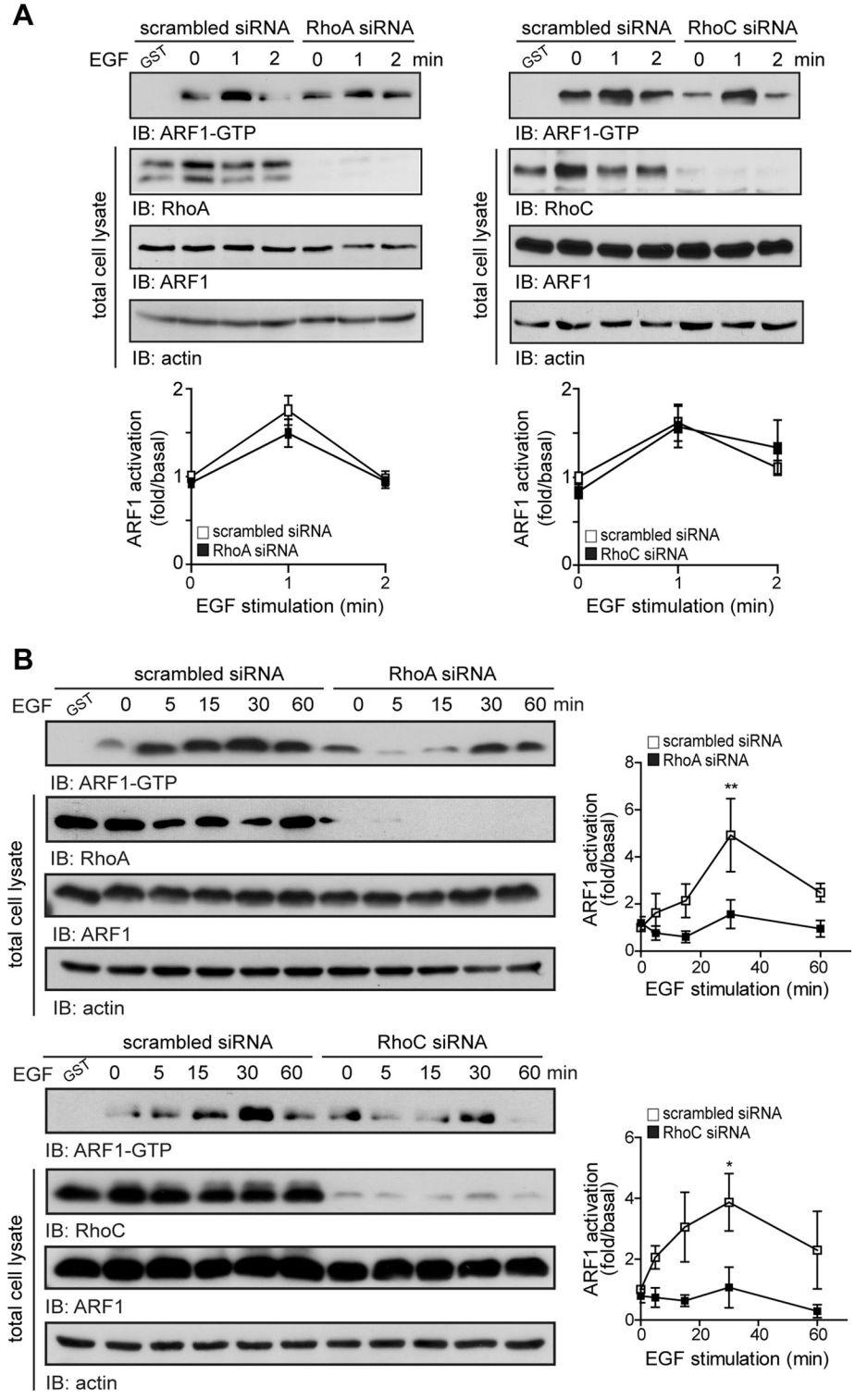


FIGURE 7: RhoA and RhoC control the late phase of ARF1 activation. MDA-MB-231 cells were transfected with a scrambled, RhoA, or RhoC siRNA and stimulated with EGF (100 ng/ml) for the indicated time. The active forms of ARF1, as well as endogenous levels of ARF1, RhoA, RhoC, and actin, were analyzed by Western blot. (A) Early time points of EGF stimulation. Quantifications are mean ± SEM of three independent experiments. (B) Longer time points of EGF stimulation. Results are mean ± SEM of three to four independent experiments. *$p < 0.05$, **$p < 0.01$ are values compared with the nonstimulated scrambled siRNA condition.

impaired maturation of invadopodia, as well as shedding of microvesicles. Although ARF1 does not localize to invadopodia, our data suggest that this ARF isoform might act as a molecular switch to coordinate the downstream signaling events important for this process by acting on the recruitment or function of key proteins involved in invadopodia maturation and stabilization. In contrast, we report that ARF1 can be found in shedding microvesicles. Over the years, numerous bioactive molecules, similar to the ones present in plasma membrane, have been found in microvesicles (Ratajczak *et al.*, 2006). These structures are known to carry signaling complexes and are considered as constituents of the tumor environment. Their role in carcinogenesis is therefore pivotal. In MDA-MB-231 cells, silencing of ARF1 reduced by 32% the amount of shedding microvesicles, suggesting that this GTPase acts, in part, to control microvesicle fission. Our data therefore indicate that ARF1 modulates breast cancer cell invasiveness by affecting the cellular structures formed to breach the matrix and associated MMP-9 activity.

Our analysis of the signaling pathway by which ARF1 controls invasion of cancer cells revealed that this particular GTPase modulates the activity of another family of small GTP-binding proteins, the Rho family. This family includes three isoforms, RhoA, RhoB, and RhoC. RhoA and RhoC are oncogenic and associated with enhanced cell proliferation and invasion, whereas RhoB has tumor suppressor properties (Sahai and Marshall, 2002; Wheeler and Ridley, 2004). The roles played by RhoA and C isoforms are believed to be distinct. RhoA regulates invasion through its ability to target MT1-MMP at the invadopodia of MDA-MB-231 cells (Sakurai-Yageta *et al.*, 2008). Alternatively, RhoC was reported to control cofilin activity at invadopodia of MTLn3 cells, a highly metastatic rat mammary adenocarcinoma cell line (Bravo-Cordero *et al.*, 2011). In MDA-MB-231 cells, ARF1, RhoA, and RhoC are highly expressed and activated upon EGF stimulation. In our cell model, we confirm that RhoA/C is also a key factor of invasion. Our results show that ARF1 controls the activity of both GTPases, thereby affecting the specific function of these two isoforms during the invasion process. This effect was further supported by the use of two other cell lines—HCC70, another triple-negative breast cancer cell line, and SKBR-3, a HER2+ breast cancer cell line—suggesting that the effect of ARF1 on RhoA/C is not cell type specific but could represent a general mechanism. It was previously suggested that ARF1 could act upstream of Rho in the context of stress fiber formation (Norman *et al.*, 1998). By demonstrating here that ARF1 and Rho GTPases can be found in complex and that depletion of this ARF abolished the ability of an extracellular stimulus to

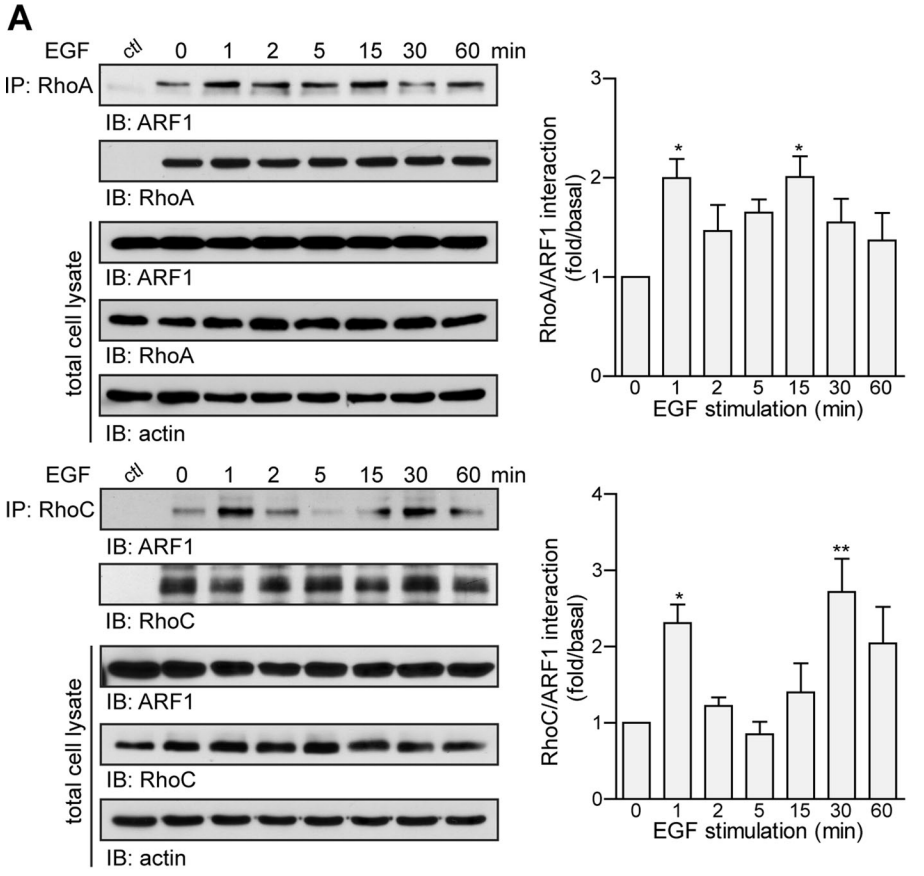


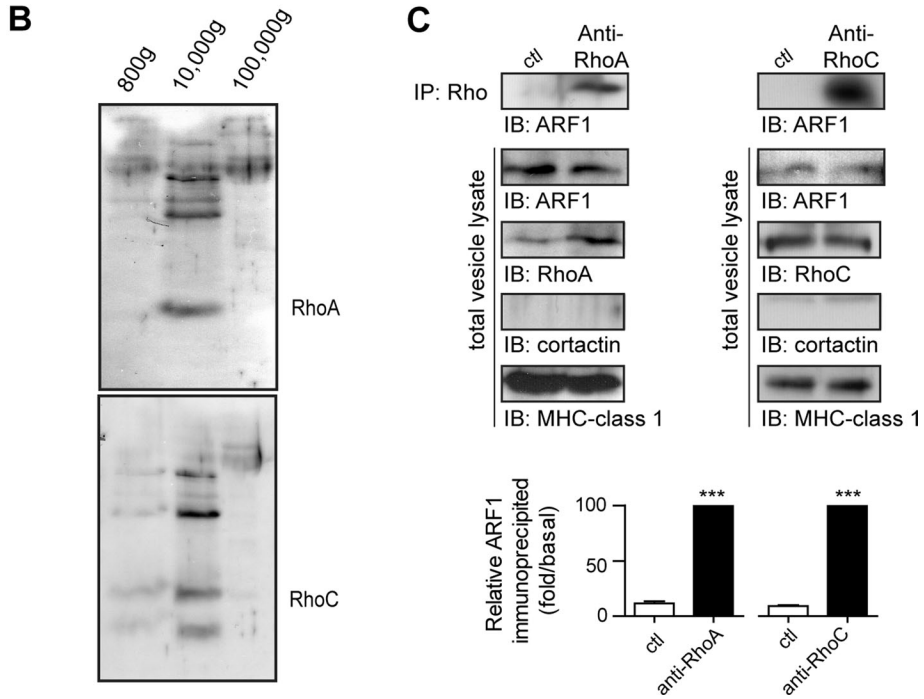


FIGURE 8: EGF stimulation promotes the association of ARF1 and Rho GTPases. (A) MDA-MB-231 cells were stimulated with EGF (100 ng/ml) for the indicated time. RhoA and RhoC were immunoprecipitated and associated ARF1 detected by Western blotting. Data are mean ± SEM of three and four experiments. *$p < 0.05$, **$p < 0.01$; values compared with the nonstimulated scrambled siRNA condition. (B) Shedding microvesicles were isolated by differential centrifugation and RhoA/C detected by Western blotting. These experiments are representative of three others. (C) RhoA and RhoC were immunoprecipitated from shedding microvesicle lysates and associated ARF1 detected by Western blotting. Control (ctl) refers to conditions in which preimmune serum was used instead of the anti-RhoA/C. MHC class 1 was used as a marker of shedding microvesicle and cortactin as a cellular marker. Results are mean ± SEM of three to four independent experiments. ***$p < 0.001$; values compared with control conditions.

activate Rho, we clearly show that ARF1 is an upstream regulator of Rho activity. Of interest, we observed a rapid and transient initial phase of activation, as well as a second sustained phase of activation, for both families of GTPases. The exact role of those two rounds of activation remains to be determined. Moreover, the association of the two GTPases occurs at time points at which both ARF1 and RhoA/C are maximally activated. Given that many signaling events, including EGFR internalization, occur after ligand binding, the localization of the pools of activated GTPases might differ. The second phase of ARF1 activation appears to be regulated in part by Rho activation, suggesting a feedback regulatory mechanism. Of interest, we observed the presence of RhoA/C in shedding microvesicles and demonstrated that in these structures, ARF1 and RhoA/C can be found in complex. In a previous report, RhoA was not detected in microvesicles of the MDA-MB-231 cell line (Li *et al.*, 2012). Our findings may be explained by a higher sensitivity of our approach.

Recently we reported that ARF1 also acts to control Rac1 activation in MDA-MB-231 cells (Lewis-Saravalli *et al.*, 2013). This GTPase is a member of the Rho family of small GTP-binding proteins and is well known for its role in cell migration. Together with the data we report here, these findings further support a central role for ARF1 in the regulation of this family of GTPases. First, depletion of ARF1 greatly impairs Rac1 activation, thereby limiting membrane targeting of IRSp53, cytoskeletal reorganization, and cell migration. Second, this ARF isoform controls Rho activity to regulate MLC phosphorylation, proteolytic activity, and invasiveness. By modulating Rac1 and RhoA/C activity, ARF1 acts as a central regulator of the two key features conferring the invasive phenotype of cancer cells. Furthermore, our previous work demonstrated that depletion of ARF1 leads to inactivation of the PI3K pathway in MDA-MB-231 cells (Boulay *et al.*, 2008). It is well documented that Rac1 activation can depend on PI3K activation (for a review, see Welch *et al.*, 2003). Similarly, different groups have reported that RhoA and

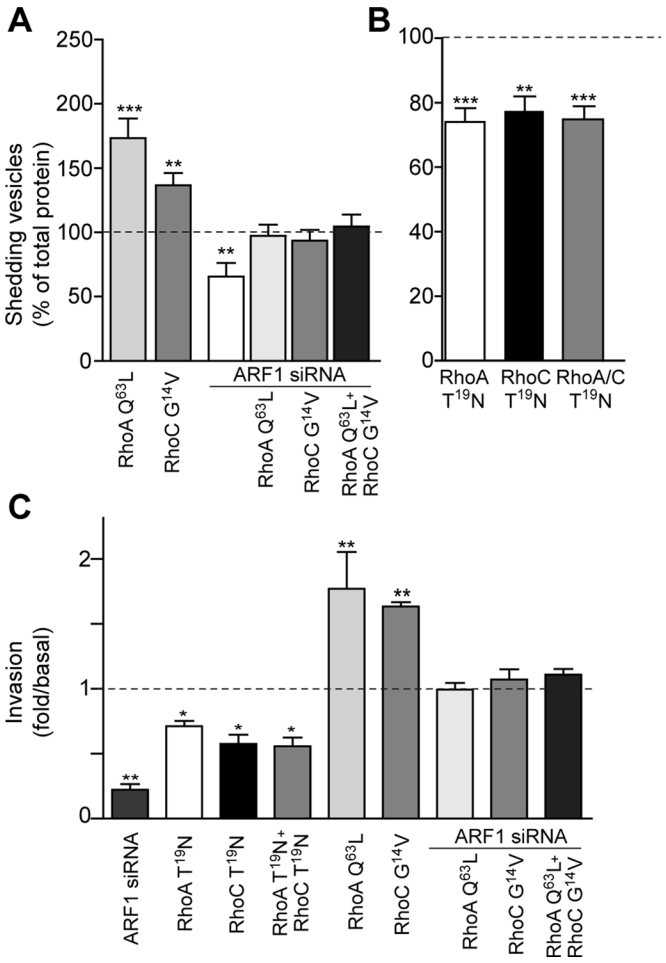


FIGURE 9: Modulation of the Rho/MLC pathway by ARF1 controls the release of shedding microvesicles. (A) Cells were transfected with constitutively active forms of RhoA and/or RhoC (RhoA $Q^{63}L$; RhoC $G^{14}V$) and a scrambled or ARF1 siRNA. The release of shedding microvesicles was quantified by assessing protein contents in all conditions. Results are mean ± SEM of three independent experiments. $^{**}p < 0.01$, $^{***}p < 0.001$; values compared with the empty vector or scrambled siRNA (dotted line). (B) Cells were transfected with the dominant-negative mutants of RhoA and/or RhoC ($T^{19}N$), and the release of shedding microvesicles was performed as in A. Results are mean ± SEM of five independent experiments. $^{**}p < 0.01$, $^{***}p < 0.001$; values compared with the empty vector control condition (dotted line). (C) Cells were transfected as in A and B and seeded into Matrigel-coated Boyden chambers. EGF (100 ng/ml) was added for a period of 20 h. Data are mean ± SEM of three experiments $^{*}p < 0.05$, $^{**}p < 0.01$; values compared with the control condition (dotted line).

RhoC activation can be regulated by the PI3K/Akt signaling axis (Qiang *et al.*, 2004; Ruth *et al.*, 2006; Kakinuma *et al.*, 2008). Together these observations suggest that ARF1 might control Rac1 and RhoA/C activation by a mechanism involving the PI3K/Akt pathway.

Taken together, our findings demonstrate that ARF proteins are key regulators of invasion. The demonstration that ARF1 regulates invasiveness complements previous reports that highlighted the role of ARF6 in this process (Hashimoto *et al.*, 2004; Tague *et al.*, 2004). This ARF isoform was reported to regulate both invadopodia formation and microvesicle shedding, although through different mechanisms (Hashimoto *et al.*, 2004; Tague *et al.*, 2004; Muralidharan-Chari *et al.*, 2009). We previously demonstrated that in MDA-MB-231 cells, EGF stimulation activates ARF1 and ARF6 to modulate, respectively, the PI3K and Erk pathways (Boulay *et al.*, 2008). This illustrates that, although the physiological endpoint might be similar, in that case cell migration, the means by which proteins regulate the events leading to that response can be different.

Our findings uncover an unsuspected new role for ARF1 in regulating key events important for cellular invasion, revealing a new potential therapeutic target for treatment of invasive breast cancers. Gaining an understanding of the molecular mechanisms by which intracellular signaling proteins control key feature of cancer cells is crucial for the development of novel therapies.

## MATERIALS AND METHODS

### Reagents and antibodies

BD Matrigel matrix was purchased from BD Bioscience (Bedford, MA). Lipofectamine 2000, fluorescein isothiocyanate–gelatin (G13187), Alexa Fluor 488–phalloidin, rhodamine–phalloidin, and Hoechst were purchased from Invitrogen (Burlington, Canada). Anti-ARF1 was obtained from ProteinTech (Chicago, IL). Anti-cortactin, anti–myosin light chain 2, anti–myosin light chain 2 Thr-18/Ser-19, anti–pan-actin, anti-cortactin, and anti-RhoC were from Cell Signaling Technology (Danvers, MA). Anti–pro-MMP-9 (IM09L) antibody was obtained from Calbiochem (Gibbstown, NJ) and anti-MMP9 from Abcam (Cambridge, MA). Anti–major histocompatibility complex class I (H300), anti-RhoA (26C4), anti–MMP-2 (H-76), anti-Ub (P4D1), and anti-Tks5 (M-300) were purchased from Santa Cruz Biotechnology (Santa Cruz, CA). All others products were from Sigma Aldrich (Oakville, Canada).

### Cell culture and transfection

MDA-MB-231, SKBR3, and HCC70 cells were obtained from Sylvie Mader (University of Montreal, Canada). MDA-MB-231 and SKBR3 cells were maintained in DMEM and HCC70 in RPMI supplemented with 10% fetal bovine serum, penicillin/streptomycin (Wisent, St-Bruno, Canada). Cells were maintained at 37°C in 5% $CO_2$. Cells were transfected with DNA and/or siRNA using Lipofectamine 2000 according to the manufacturer's instructions. ARF1 siRNA used throughout this study was designed against part of the 3′ untranslated region and coding region of ARF1; ARF1 siRNA 2 used in Supplemental Figures S1 and S3 was designed against the C-terminal coding region. ARF1 and scrambled siRNA were synthesized by Thermo Science Dharmacon (Lafayette, CO). DNA used were pRK5, pcDNA 3.1, RhoA $T^{19}$N-myc (gift from S. Offermanns, University of Heidelberg, Heidelberg, Germany), RhoC $T^{19}$N-HA (Missouri S&T cDNA Research Center, Rolla, MO), ARF1-HA (gift from N. Vitale, Université de Strasbourg, Strasbourg, France), and ARF1 $T^{31}$N and ARF1 $Q^{71}$L (gift from J. Presley, McGill University, Montreal, Canada). For rescue experiments, ARF1-HA was transfected 24 h after introduction of the ARF1 siRNA 1.

### Invasion and migration assays

Cells were transfected with siRNA (72 h) and serum starved before the assay. Briefly, cells were trypsinized and seeded into Boyden chambers (24-well inserts with 8-μm pore, precoated with Matrigel). One hour after plating, cells were stimulated with EGF (30 ng/ml). After 20 h, cells were fixed using 4% paraformaldehyde and incubated with 0.1% crystal violet. Membranes were washed with phosphate-buffered saline (PBS), and cells present in the upper chamber were removed using a cotton swab. The number of cells in the lower chamber was counted manually under a phase contrast

microscope. Pictures were taken using an inverted Leica microscope (Leica, Wetzlar, Germany). Relative migration was quantified using ImageJ (National Institutes of Health, Bethesda, MD). For the migration assays, the experiments were done as described, using uncoated Boyden chambers.

### Three-dimensional morphogenesis

Cells were plated into Matrigel-coated 48-well plate 48 h after transfection with scrambled or ARF1 siRNAs. Cultures were overlaid with media containing 2.5% Matrigel and grown for 5 d as previously done (Debnath *et al.*, 2002; Lee *et al.*, 2007). Cell colonies were defined as being either stellate or spheroidal. A colony was deemed stellate if one or more projections from the central sphere of cells were observed. Images were taken on an inverted microscope (Leica).

### Gelatin degradation

Coverslips were coated with poly-L-lysine and fixed with glutaraldehyde. The slides were then covered with 500 µl of Alexa Fluor 488–coupled gelatin (0.02% porcine gelatin Alexa Fluor 488, 0.1% porcine gelatin, 0.2% sucrose; Invitrogen) for 3 h at 37°C in the dark. Slides were sterilized with ethanol, rinsed with PBS, and left in media. Cells were added and left to adhere for 16 h. The cells were then labeled with rhodamine–phalloidin and immunofluorescence observed using a confocal microscope (LSM510META; Carl Zeiss, Jena, Germany). For real-time imaging, cells were seeded onto a glass-bottom Petri dish (MatTek, Ashland, MA) in Leibovitz's 15 media (Invitrogen). Pictures were taken after 1 h to give cells time to spread. The ambient temperature was maintained at 37°C with a thermostated sealed chamber around the confocal microscope. Pictures were taken using a confocal microscope (LSM510META).

### Microscopy

The cells were fixed with PBS solution containing 4% paraformaldehyde for 15 min at room temperature and then permeabilized with a solution of DMEM containing 0.05% saponin. The slides were incubated for 1 h with a primary antibody. After several washes, the plates were incubated for 1 h in the dark in the presence of an anti-mouse or anti-rabbit Alexa Fluor 488 antibody (Invitrogen). Cells were then mounted on slides using a solution of Aqua-mount (Fisher Scientific, Ottawa, Canada) and observed using a confocal microscope (LSM510META).

### Microvesicle isolation

Cells were first seeded in 15-cm dishes. After 3 d, medium was carefully removed and subjected to differential centrifugations (800 × *g*, 10 min; 10,000 × *g*, 30 min, 100,000 × *g*, 60 min) as previously described (Muralidharan-Chari *et al.*, 2009). Isolated microvesicles were washed in PBS and lysed in Triton, glycerol, HEPES (TGH) buffer (Boulay *et al.*, 2008). Protein content was assessed using a bicinchoninic acid protein assay and normalized from total cell lysate (Fisher).

### Electron microscopy

The 10,000 × *g* pellet from the cell culture supernatant was fixed by immersion in 1% glutaraldehyde in 0.1 M phosphate buffer (pH 7.4) for 2 h and embedded in Epon (K4M CANEMCO; St-Laurent, Canada). Thin sections (70–100 nm) of pellets were mounted on nickel-coated grids. Samples were processed as previously described (Bendayan, 1995). First, the samples were incubated with 1% ovalbumin, then with the anti-ARF1 antibody for 2 h, and finally with the protein A–gold complex (10 nm) for 30 min at room temperature. Control experiments to assess the specificity of the immunogold were performed by omitting the anti-ARF1 antibody. Sections were thoroughly washed with PBS/$H_2O$. Samples were counterstained with uranyl acetate and examined using a transmission electron microscope (CM 100; Philips/FEI, Hillsboro, OR).

### Rho activation

Cells were transfected with scrambled or ARF1 siRNAs (50 nM), and activation of Rho was performed as previously described (Piekny and Glotzer, 2008). Briefly, cells were washed with Tris-buffered saline (TBS) and lysed in 300 µl of ice-cold MLB lysis buffer (25 mM 4-(2-hydroxyethyl)-1-piperazineethanesulfonic acid, 150 mM NaCl, 1% Nonidet P-40, 10 mM $MgCl_2$, 1 mM EDTA, 10% glycerol, and 0.3 mg/ml phenylmethylsulfonyl fluoride complemented with protease inhibitors and 1 nM sodium orthovanadate). Samples were vortexed for 10 s and spun for 10 min at 10,000 × *g*. Glutathione *S*-transferase (GST)–Rhotekin coupled to glutathione Sepharose 4B was added to each tube, and samples were rotated at 4°C for 90 min. Beads were washed, and proteins were eluted in 25 µl of SDS sample buffer by heating to 65°C for 15 min. Detection of Rho-GTP was performed by immunoblot analysis using a specific anti-RhoA or anti-RhoC antibody.

### ARF1 activation

Cells transfected with scrambled, RhoA, or RhoC (50 nM) siRNAs were washed with TBS and lysed in 300 µl of ice-cold MLB lysis buffer. Samples were vortexed for 10 s and spun for 10 min at 10,000 × *g*. GST-GGA3 coupled to glutathione Sepharose 4B was added to each tube, and samples were rotated at 4°C for 45 min. Beads were washed, and proteins were eluted in 25 µl of SDS sample buffer by heating to 65°C for 15 min. Detection of ARF1-GTP was performed by immunoblot analysis using a specific anti-ARF1 antibody.

### Coimmunoprecipitation

MDA-MB-231 cells were serum starved overnight and stimulated with EGF (100 ng/ml) for the indicated times. Coimmunoprecipitation experiments were described previously (Cotton *et al.*, 2007). Briefly, cells were lysed into TGH buffer, and RhoA or RhoC were immunoprecipitated using the anti-RhoA or anti-RhoC antibody. Interacting ARF1 was assessed by Western blot analysis.

### Western blotting

Cells were harvested, and total soluble proteins were run on polyacrylamide gels and transferred onto nitrocellulose membranes. The membranes were blotted for relevant proteins using specific primary antibodies (as described for each experiment). Secondary antibodies were FITC or horseradish peroxidase conjugated, and fluorescence was detected using a Typhoon 9410 scanner (GE Healthcare Life Sciences, Piscataway, NJ) or with enhanced chemiluminescence detection reagent. Quantification of the digital images obtained was performed using ImageQuant 5.2 software (GE Healthcare Life Sciences).

### Gelatin zymography

Zymography assays were performed as previously described (Chavey *et al.*, 2003). To assess MMP activity in cell supernatant, cells were first serum starved for 12 h. The supernatant was recovered and concentrated using Microcon tube (Cedarlane, Burlington, Canada). Samples were mixed with nondenaturing SDS-sample buffer and migrated on a 10% polyacrylamide gel containing 0.1% gelatin. To assess MMP activity in the microvesicles, microvesicle lysates (described previously) were directly incubated with nondenaturing SDS-sample buffer and migrated on a 10% polyacrylamide gel

containing 0.1% gelatin as for the whole supernatant experiments. The gel was then incubated twice for 30 min in a 3.5% Triton solution. Once the enzymes partially renatured, the gels were incubated overnight in a solution of Brij (0.02% polyoxyethylene 20 cetyl ether, 5 mM $CaCl_2$, 200 mM NaCl, 50 mM Tris-HCl, pH 7.4) containing or not containing a broad-spectrum inhibitor, batimastat (BB-94; 10 μM). Gels were stained for 10 min with Coomassie blue and then washed for several hours (5% acetic acid, 10% methanol). Enzymatic activities appear as cleared bands on a dark background.

### RNA extraction

Total RNA was extracted from MDA-MB-231 with TRIzol reagent (Life Technologies, Carlsbad, CA) according to the manufacturer's instructions. Real time-PCR was performed by the genomic platform at the Institut de Recherche en Immunologie et en Cancérologie's Genomics Core Facility (Montreal, Canada).

### 3-(4,5-Dimethylthiazol-2-yl)-2,5-diphenyl tetrazolium bromide assay

The number of proliferative cells was measured by 3-(4,5-dimethylthiazol-2-yl)-2,5-diphenyl tetrazolium bromide (MTT) assay. Briefly, cells were cultured in DMEM in 96-well plates ($1 \times 10^4$ cells/well), left untreated (nonstimulated), or stimulated with EGF. After 20 h, cells were incubated with 20 μl of MTT (5 mg/ml) for an additional 4 h at 37°C, after which the crystals were dissolved using a dissolving buffer (50% SDS and 50% dimethyl foramide [DMF]). After complete dissolution of the crystals, the absorbance at 570 nm was immediately measured on a microplate reader (Wallac Victor; Perkin Elmer, MA).

### Statistical analysis

Statistical analyses were performed using one-way analysis of variance followed by Bonferroni's multiple comparison tests or *t* test using Prism, version 4.0a (GraphPad, San Diego, CA).

## ACKNOWLEDGMENTS

We thank D. Gingras from the electron microscopy facility of the Université de Montréal. We are grateful to Cyril Bignone (independent 3D artist, Montréal, Canada) for conception of the synthesis video and Eric Haines (Université de Montréal) for voice narration. We thank Stéphane A. Laporte (McGill University, Montréal, Canada) for the use of his confocal microscope. This work was supported by the Canadian Institutes of Health Research (MOP-106596 to A.C.). A.C. is the recipient of a Senior Scientist Award from the Fonds de Recherche du Québec-Santé.

## REFERENCES

Alexander NR, Branch KM, Parekh A, Clark ES, Iwueke IC, Guelcher SA, Weaver AM (2008). Extracellular matrix rigidity promotes invadopodia activity. Curr Biol 18, 1295–1299.

Amano M, Ito M, Kimura K, Fukata Y, Chihara K, Nakano T, Matsuura Y, Kaibuchi K (1996). Phosphorylation and activation of myosin by Rho-associated kinase (Rho-kinase). J Biol Chem 271, 20246–20249.

Bendayan M (1995). Colloidal gold post-embedding immunocytochemistry. Prog Histochem Cytochem 29, 1–159.

Boulay PL, Cotton M, Melancon P, Claing A (2008). ADP-ribosylation factor 1 controls the activation of the phosphatidylinositol 3-kinase pathway to regulate epidermal growth factor-dependent growth and migration of breast cancer cells. J Biol Chem 283, 36425–36434.

Boulay PL, Schlienger S, Lewis-Saravalli S, Vitale N, Ferbeyre G, Claing A (2011). ARF1 controls proliferation of breast cancer cells by regulating the retinoblastoma protein. Oncogene 30, 3846–3861.

Bravo-Cordero JJ, Oser M, Chen X, Eddy R, Hodgson L, Condeelis J (2011). A novel spatiotemporal RhoC activation pathway locally regulates cofilin activity at invadopodia. Curr Biol 21, 635–644.

Brown PD (1995). Matrix metalloproteinase inhibitors: a novel class of anticancer agents. Adv Enzyme Regul 35, 293–301.

Chavey C, Mari B, Monthouel MN, Bonnafous S, Anglard P, Van Obberghen E, Tartare-Deckert S (2003). Matrix metalloproteinases are differentially expressed in adipose tissue during obesity and modulate adipocyte differentiation. J Biol Chem 278, 11888–11896.

Clark EA, Golub TR, Lander ES, Hynes RO (2000). Genomic analysis of metastasis reveals an essential role for RhoC. Nature 406, 532–535.

Cocucci E, Racchetti G, Meldolesi J (2009). Shedding microvesicles: artefacts no more. Trends Cell Biol 19, 43–51.

Cohen LA, Honda A, Varnai P, Brown FD, Balla T, Donaldson JG (2007). Active Arf6 recruits ARNO/cytohesin GEFs to the PM by binding their PH domains. Mol Biol Cell 18, 2244–2253.

Cotton M, Boulay PL, Houndolo T, Vitale N, Pitcher JA, Claing A (2007). Endogenous ARF6 interacts with Rac1 upon angiotensin II stimulation to regulate membrane ruffling and cell migration. Mol Biol Cell 18, 501–511.

Debnath J, Mills KR, Collins NL, Reginato MJ, Muthuswamy SK, Brugge JS (2002). The role of apoptosis in creating and maintaining luminal space within normal and oncogene-expressing mammary acini. Cell 111, 29–40.

Dolo V, D'Ascenzo S, Violini S, Pompucci L, Festuccia C, Ginestra A, Vittorelli ML, Canevari S, Pavan A (1999). Matrix-degrading proteinases are shed in membrane vesicles by ovarian cancer cells in vivo and in vitro. Clin Exp Metastasis 17, 131–140.

D'Souza-Schorey C, Chavrier P (2006). ARF proteins: roles in membrane traffic and beyond. Nat Rev Mol Cell Biol 7, 347–358.

Fritz G, Brachetti C, Bahlmann F, Schmidt M, Kaina B (2002). Rho GTPases in human breast tumours: expression and mutation analyses and correlation with clinical parameters. Br J Cancer 87, 635–644.

Gilcrease MZ, Zhou X, Lu X, Woodward WA, Hall BE, Morrissey PJ (2009). Alpha6beta4 integrin crosslinking induces EGFR clustering and promotes EGF-mediated Rho activation in breast cancer. J Exp Clin Cancer Res 28, 67.

Hashimoto S, Onodera Y, Hashimoto A, Tanaka M, Hamaguchi M, Yamada A, Sabe H (2004). Requirement for Arf6 in breast cancer invasive activities. Proc Natl Acad Sci USA 101, 6647–6652.

Hegedus L, Cho H, Xie X, Eliceiri GL (2008). Additional MDA-MB-231 breast cancer cell matrix metalloproteinases promote invasiveness. J Cell Physiol 216, 480–485.

Ho WT, Exton JH, Williger BT (2003). Arfaptin 1 inhibits ADP-ribosylation factor-dependent matrix metalloproteinase-9 secretion induced by phorbol ester in HT 1080 fibrosarcoma cells. FEBS Lett 537, 91–95.

Huveneers S, Danen EH (2009). Adhesion signaling—crosstalk between integrins, Src and Rho. J Cell Sci 122, 1059–1069.

Kakinuma N, Roy BC, Zhu Y, Wang Y, Kiyama R (2008). Kank regulates RhoA-dependent formation of actin stress fibers and cell migration via 14–3-3 in PI3K-Akt signaling. J Cell Biol 181, 537–549.

Karnoub AE, Weinberg RA (2008). Ras oncogenes: split personalities. Nat Rev Mol Cell Biol 9, 517–531.

Kelly T, Yan Y, Osborne RL, Athota AB, Rozypal TL, Colclasure JC, Chu WS (1998). Proteolysis of extracellular matrix by invadopodia facilitates human breast cancer cell invasion and is mediated by matrix metalloproteinases. Clin Exp Metastasis 16, 501–512.

Kimura K *et al.* (1996). Regulation of myosin phosphatase by Rho and Rho-associated kinase (Rho-kinase). Science 273, 245–248.

Lee GY, Kenny PA, Lee EH, Bissell MJ (2007). Three-dimensional culture models of normal and malignant breast epithelial cells. Nat Methods 4, 359–365.

Lewis-Saravalli S, Campbell S, Claing A (2013). ARF1 controls Rac1 signaling to regulate migration of MDA-MB-231 invasive breast cancer cells. Cell Signal 25, 1813–1819.

Li B, Antonyak MA, Zhang J, Cerione RA (2012). RhoA triggers a specific signaling pathway that generates transforming microvesicles in cancer cells. Oncogene 31, 4740–4749.

Li L, Chen P, Ling Y, Song X, Lu Z, He Q, Li Z, Lu N, Guo Q (2011). Inhibitory effects of GL-V9 on the invasion of human breast carcinoma cells by downregulating the expression and activity of matrix metalloproteinase-2/9. Eur J Pharm Sci 43, 393–399.

Mardilovich K, Olson MF, Baugh M (2012). Targeting Rho GTPase signaling for cancer therapy. Future Oncol 8, 165–177.

Molli PR, Adam L, Kumar R (2008). Therapeutic IMC-C225 antibody inhibits breast cancer cell invasiveness via Vav2-dependent activation of RhoA GTPase. Clin Cancer Res 14, 6161–6170.

Monsky WL, Lin CY, Aoyama A, Kelly T, Akiyama SK, Mueller SC, Chen WT (1994). A potential marker protease of invasiveness, seprase, is localized on invadopodia of human malignant melanoma cells. Cancer Res 54, 5702–5710.
Muralidharan-Chari V, Clancy J, Plou C, Romao M, Chavrier P, Raposo G, D'Souza-Schorey C (2009). ARF6-regulated shedding of tumor cell-derived plasma membrane microvesicles. Curr Biol 19, 1875–1885.
Muralidharan-Chari V, Clancy JW, Sedgwick A, D'Souza-Schorey C (2010). Microvesicles: mediators of extracellular communication during cancer progression. J Cell Sci 123, 1603–1611.
Murphy DA, Courtneidge SA (2011). The "ins" and "outs" of podosomes and invadopodia: characteristics, formation and function. Nat Rev Mol Cell Biol 12, 413–426.
Nakahara H, Howard L, Thompson EW, Sato H, Seiki M, Yeh Y, Chen WT (1997). Transmembrane/cytoplasmic domain-mediated membrane type 1-matrix metalloprotease docking to invadopodia is required for cell invasion. Proc Natl Acad Sci USA 94, 7959–7964.
Norman JC, Jones D, Barry ST, Holt MR, Cockcroft S, Critchley DR (1998). ARF1 mediates paxillin recruitment to focal adhesions and potentiates Rho-stimulated stress fiber formation in intact and permeabilized Swiss 3T3 fibroblasts. J Cell Biol 143, 1981–1995.
Piekny AJ, Glotzer M (2008). Anillin is a scaffold protein that links RhoA, actin, and myosin during cytokinesis. Curr Biol 18, 30–36.
Pille JY *et al.* (2005). Anti-RhoA and anti-RhoC siRNAs inhibit the proliferation and invasiveness of MDA-MB-231 breast cancer cells in vitro and in vivo. Mol Ther 11, 267–274.
Qiang YW, Yao L, Tosato G, Rudikoff S (2004). Insulin-like growth factor I induces migration and invasion of human multiple myeloma cells. Blood 103, 301–308.
Ratajczak J, Wysoczynski M, Hayek F, Janowska-Wieczorek A, Ratajczak MZ (2006). Membrane-derived microvesicles: important and underappreciated mediators of cell-to-cell communication. Leukemia 20, 1487–1495.
Ruth MC, Xu Y, Maxwell IH, Ahn NG, Norris DA, Shellman YG (2006). RhoC promotes human melanoma invasion in a PI3K/Akt-dependent pathway. J Invest Dermatol 126, 862–868.
Sabe H, Hashimoto S, Morishige M, Ogawa E, Hashimoto A, Nam JM, Miura K, Yano H, Onodera Y (2009). The EGFR-GEP100-Arf6-AMAP1 signaling pathway specific to breast cancer invasion and metastasis. Traffic 10, 982–993.
Sahai E, Marshall CJ (2002). RHO-GTPases and cancer. Nat Rev Cancer 2, 133–142.
Sakurai-Yageta M, Recchi C, Le Dez G, Sibarita JB, Daviet L, Camonis J, D'Souza-Schorey C, Chavrier P (2008). The interaction of IQGAP1 with the exocyst complex is required for tumor cell invasion downstream of Cdc42 and RhoA. J Cell Biol 181, 985–998.
Seals DF, Azucena EF Jr, Pass I, Tesfay L, Gordon R, Woodrow M, Resau JH, Courtneidge SA (2005). The adaptor protein Tks5/Fish is required for podosome formation and function, and for the protease-driven invasion of cancer cells. Cancer Cell 7, 155–165.
Simpson KJ, Dugan AS, Mercurio AM (2004). Functional analysis of the contribution of RhoA and RhoC GTPases to invasive breast carcinoma. Cancer Res 64, 8694–8701.
Stylli SS, Stacey TT, Verhagen AM, Xu SS, Pass I, Courtneidge SA, Lock P (2009). Nck adaptor proteins link Tks5 to invadopodia actin regulation and ECM degradation. J Cell Sci 122, 2727–2740.
Suwa H, Ohshio G, Imamura T, Watanabe G, Arii S, Imamura M, Narumiya S, Hiai H, Fukumoto M (1998). Overexpression of the rhoC gene correlates with progression of ductal adenocarcinoma of the pancreas. Br J Cancer 77, 147–152.
Tague SE, Muralidharan V, D'Souza-Schorey C (2004). ADP-ribosylation factor 6 regulates tumor cell invasion through the activation of the MEK/ERK signaling pathway. Proc Natl Acad Sci USA 101, 9671–9676.
Taraboletti G, D'Ascenzo S, Borsotti P, Giavazzi R, Pavan A, Dolo V (2002). Shedding of the matrix metalloproteinases MMP-2, MMP-9, and MT1-MMP as membrane vesicle-associated components by endothelial cells. Am J Pathol 160, 673–680.
Vigil D, Cherfils J, Rossman KL, Der CJ (2010). Ras superfamily GEFs and GAPs: validated and tractable targets for cancer therapy. Nat Rev Cancer 10, 842–857.
Weaver AM (2006). Invadopodia: specialized cell structures for cancer invasion. Clin Exp Metastasis 23, 97–105.
Welch HC, Coadwell WJ, Stephens LR, Hawkins PT (2003). Phosphoinositide 3-kinase-dependent activation of Rac. FEBS Lett 546, 93–97.
Wheeler AP, Ridley AJ (2004). Why three Rho proteins? RhoA, RhoB, RhoC, and cell motility. Exp Cell Res 301, 43–49.
Wu M, Wu ZF, Rosenthal DT, Rhee EM, Merajver SD (2010). Characterization of the roles of RHOC and RHOA GTPases in invasion, motility, and matrix adhesion in inflammatory and aggressive breast cancers. Cancer 116, 2768–2782.
Yonemura S, Hirao-Minakuchi K, Nishimura Y (2004). Rho localization in cells and tissues. Exp Cell Res 295, 300–314.